

## Assessing the Reliability of New Connector Designs

Heather McCormick and George Riccitelli  
Celestica Inc.  
Toronto, ON, Canada

### Abstract

With the combination of increased product complexity, increased frequencies and ever decreasing component sizes and pitches designers are faced with the dilemma on how design their products in the most cost effective manner possible. In larger more complex products designers most often than not are creating “islands of densities” or daughter cards that join onto larger and more complex boards. In order for designers to “link” the daughter cards to the motherboard designers are using newly designed interconnect products. Interconnect suppliers have introduced products such as a BGA type board to board connector. Advantages of this type of connector extend into the contract manufacturing realm as the connectors are processed during the mass reflow of the assembly eliminating process steps such as wave solder or press fit operations. The manufacturability of these connectors have been evaluated and documented in earlier reports but little data is available on the second level testing and reliability of these connectors. This report focuses on the manufacturability and reliability of the interconnects generated from accelerated thermal cycling of the “Metropolis” test vehicle (connector test vehicle). The tests were performed using IPC-9701 as a guideline. The “Metropolis” test vehicle is populated with two styles of a BGA mezzanine connector, a BGA mounted socket and two press fit connectors.

### Background

As operating frequencies increase, traditional interconnect methods are less common due to the ability of maintaining good signal integrities through the product. The signal integrities are being jeopardized due to inductance produced by the through vias on the printed wiring board and the interconnect device.

With combination of board design and new insulating materials implemented in new generation press fit connectors designers are able to overcome such hurdles. Connectors such as the surface mount area arrays not only lower inductance but allow contract manufacturer’s to eliminate a process step by attaching the connectors to the printed wiring board during mass reflow of other SMT components. Many area array interconnects are utilized to create “islands of density”. In these “islands” high speed signals are processed on smaller boards “daughter cards” and then sent back to the main board for further processing. In utilizing the interconnect solution the designer has increased flexibility and cost savings by not utilizing a printed wiring board with buildup layers (microvias). As these connectors become more widely used manufacturing data, reliability and experiences are undefined. In this paper we attempt to share our experiences and difficulties as we progressed through this project.

### Introduction

As in all new packages, reliability data must be produced. This data is usually gathered by the manufacturer and possibly reassessed by the end user. Depending on the intended end use application, common reliability tests may include torque tests, vibration tests, and/or accelerated thermal cycling. For press fit connectors used in products such as telecom equipment, reliability requirements might include Telcordia GR-1217 compliance. For a component such as flip chip ball grid array packages (FCBGAs), reliability is typically evaluated using the guidelines set out in IPC-9701[2]. Since these specifications were created, the landscape of the inconnect world has changed vastly-a new class of connectors which bridges the connector world and the BGA world has emerged – Ball Grid Array Connectors. While typical connector reliability concerns certainly continue to apply, BGA failure mechanisms must also be a concern to potential end users, and must be evaluated. The “Metropolis” test vehicle was designed to assess the reliability of BGA Connectors and newly emerging press fit connectors.

### Component Selection

As in all tests, component selection was first determined. Interconnects chosen for the test vehicle was a mixture of recent product releases and suggestions from our OEM customers. Preference was given to SMT connectors, particularly BGA connectors, connectors capable of handling high data rates. BGA connectors are still an emerging component type [3], but existing versions have proven popular in many applications. Contract manufacturers prefer the BGA attach method, as it eliminates process steps such as wave soldering, which in turn, omits the need for wave soldering equipment, and the use of associated wave pallets. This type of interconnect is also more advantageous to use than press fit type connectors as BGA connectors will be assembled and reflowed during the mass reflow of other SMT components. In a press fit type connector, the need for a mechanical press is required. BGA connectors also have the inherent benefit of area array components to self center, which is very accommodating in a manufacturing environment. With the exponential demand of increased data rates

in today’s networking and telecommunication products [4], great demands are being placed on the interconnect suppliers to quench this demand. BGA components can be helpful in this regard, due to the relatively low inductance of the BGA connection. Two different BGA board to board connectors were selected, with two different stack heights. This connector was available in several different heights; we decided to evaluate whether the stack height would have an effect on the reliability of the components, and whether the tallest versions would integrate easily into the standard assembly process. A socket for a PGA processor, which attached to the board by solder balls similar to a BGA, was also selected. Sockets are very effective in applications such as the attachment of processors where future upgrades are required. In this application, easy removal and replacement of components is possible on boards that have been previously assembled. The final components selected were two new press fit connector designs, both capable of handling data rates in excess of 6Gbps. With the ROHS initiative rapidly approaching, lead free versions of these connectors were also of great interest, but at the time of design, only one connector, the Backplane A connector was available. The study of lead free area array packages is planned on a separate project.

The “Metropolis” test vehicle contains 5 connector types as outlined in Table 1 below.

**Table 1 - Connectors Selected for Evaluation**

Connector	Technology	I/O	Pitch
Backplane A	Press Fit	192	1.8mm x 1.35mm (plug) 1.8mm x 1.8 mm(receptacle)
Backplane B	Press Fit	120	2.5 mm x 1.5 mm
Socket	BGA	700	1.27 mm
Mezzanine A	BGA	666	1 mm x 1.3 mm
Mezzanine B	BGA	300	1.27 mm

In addition to the various connector types and sizes, the project also attempts to assess the impact of various surface finishes on the connectors’ reliability. Three finishes – OSP, ENIG and Immersion Silver – were selected for in this study. Forced reworks were also part of the test matrix. Including rework in the test matrix would allow us the opportunity of assessing any impediments that may be encountered during the removal and replacement process. Furthermore, it would allow us to gather important reliability data and compare it to the initial attach data. Figure 1 outlines the test plan and quantities for the “Metropolis” project.

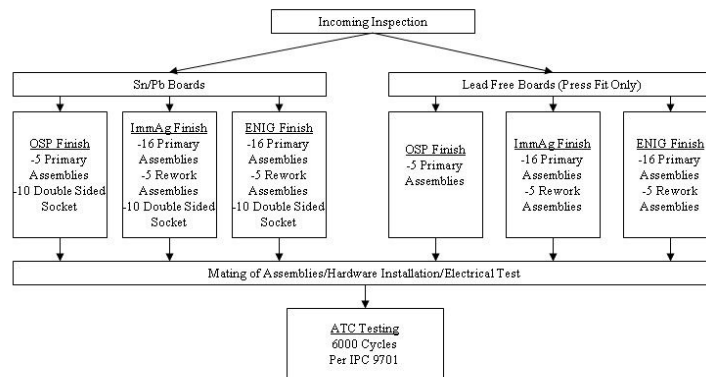


**Figure 1: Test plan for “Metropolis” project**

**Metropolis Test Vehicle Design**

Figure 2 shows the fully assembled “Metropolis” test vehicle. For a typical packaged component reliability test, the requirements for test vehicle design are governed by IPC-9701. That specification, was not, however, written with BGA connectors in mind. Regardless, many of the primary considerations do not change, and this specification remains a useful starting point in designing test vehicles and test plans for evaluating BGA connector reliability. One of the main differences is in the implementation of daisy chains through the components to be studied. In designing test vehicles for traditional BGA packages, a daisy chained version of the package to be tested is obtained from the supplier. These packages are then mounted

on a test vehicle that is designed to connect the daisy chain links inside the package to form a continuous loop through the board and component. In evaluating connectors daisy chained versions of the component are usually not available. Therefore, actual production parts are used; the daisy chain must be created entirely within the test vehicle boards. For example, in order to evaluate a mezzanine board to board connector, two different printed circuit boards must be used – one for motherboard and the other for the daughter card. Once the test vehicles were assembled, a complete daisy chain circuit through the connector and the two PCBs is created, which allows resistance measurements to be made during accelerated thermal cycling. For the socket that was selected, a set of dummy, daisy chained processor modules were obtained from the module designer to complete the daisy chains.

The Motherboard is shown in Figure 3, and the Mezzanine card and the Backplane are shown in Figure 4.

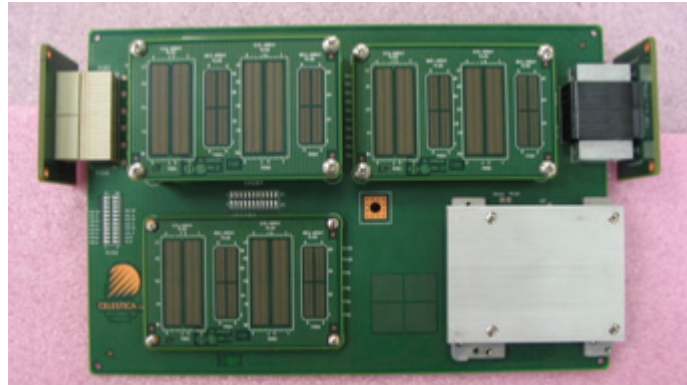


**Figure 2 - Assembled “Metropolis” Test Vehicle**

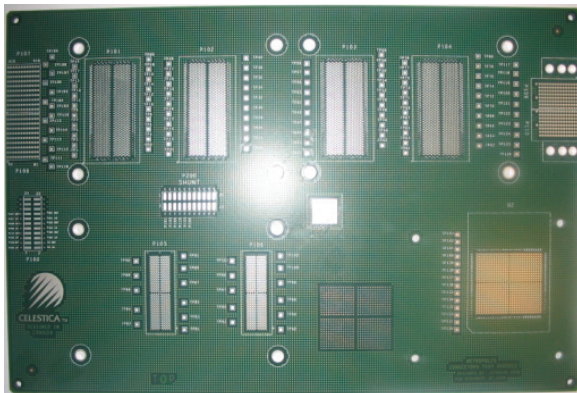


**Figure 3 - Metro Motherboard**

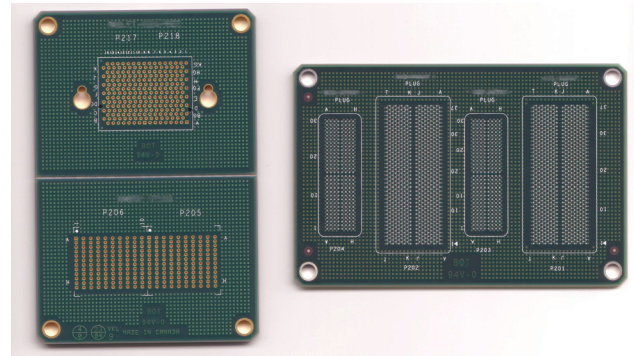


**Figure 4 - Backplane Card and Mezzanine Card**

In a typical BGA test vehicle, components would be affected by the thickness of the test vehicle on which it is assembled. For a BGA connector test vehicle, the situation is further complicated by the need to mate the two connector halves. The board thickness (or other design features) of both the motherboard and the Mezzanine card could adversely affect the reliability of the connector. All failures were electrically isolated during ATC to determine failure location(s). Depending on the final results and the locations of the failures, it may be desirable on future builds to use the same thickness and stackup for both the motherboard and the mezzanine cards in order to provide a common set of conditions for the plug and the receptacle.

The test vehicle was designed in a manner that allowed sufficient spacing between the components on the daughter cards. As well, adequate air circulation around the components was maintained on the test assemblies during accelerated thermal cycling. In most cases, two of each connector selected were placed on the card to allow fewer cards to be built for a given sample size.

Several features were added to the test vehicle to facilitate reliability testing. Test points were used to subdivide the daisy chains into shorter sub-sections, which facilitate failure isolation once components have failed in accelerated thermal cycling. The ability to jumper past failing components allowed more than one component to be placed on a single daisy chain,

allowing a smaller number of in-situ monitoring channels to be used to reduce the cost of the test. The monitoring headers used on the test vehicle were SMT pin headers, which allowed the test vehicles to be assembled without the need for wave soldering, which simplifies the assembly process.

The final unique consideration for this test vehicle was the elaborate hardware associated with the socket assembly. With chamber space at a premium and pressure to keep project costs down, it was decided to design a simple aluminium plate to mimic the complex and costly heatsink. In addition to the socket itself and the processor module, a heat sink assembly had to be considered. In order to dissipate the considerable heat generated by the processor during normal product operation, a large heat sink was mounted onto a specially designed metal frame. This frame is riveted to the board around the socket. It was imperative to maintain the effect of the heat sink assembly during the reliability testing; the heat sink assembly culminates a compression load to the top of the processor module that was connected to the socket assembly. The metal frame in its received state was too large, rather than designing a larger test vehicle we decided to alter the mounting frame from its original form. The mounting frame for the heat sink was cut so that only the portion required for this test was used. It was mounted around the socket with plastic rivets designed for production use. While the processor modules used in the test were daisy chained, the heat dissipation function of the heat sink was not required during our tests.

## **Experimental Work**

### **Test Plan**

Three surface finishes were selected for the study. As required by IPC-9701, OSP was included as a baseline. IPC-9701 also permits the use of HASL as a surface finish, but this was not used due to its incompatibility with lead free assembly. Some of the press fit portions of this evaluation will be duplicated with lead free versions of one connector, so it was decided to choose only finishes that could be used with lead free. In addition to OSP, immersion silver and electroless nickel/immersion gold were included. For the SMT components, the primary objective was to collect reliability data through accelerated thermal cycling (ATC). For the press fit connectors, the primary goal is to measure insertion and retention forces, and compare them for tin/lead and pure tin plated leads. Performance in accelerated thermal cycling will be used as a relative measure of reliability. Although ATC is typically used to accelerate the fatigue failure of solder joints, it is a relevant test for press fit joints as well. While there are many possible failure modes for press fit contacts, fretting corrosion is one that may be accelerated by thermal cycling. Micro motion at the contact interface induced by, in this case, changes in temperature, can cause wear, which can eventually lead to an increase in contact resistance. These increases can be detected by the in-situ monitoring equipment, and can give a sense of the relative performance of the connectors on different surface finishes, and also be used to compare the performance of the tin-lead plated connectors with that of the lead free connectors. Secondary goals include collection of a limited set of torque and vibration data for the BGA socket.

### **Assembly**

#### **Screening**

The motherboards and BGA connector daughter cards were assembled using a 63/37 tin/lead solder paste. Cards were screened using a 6 mil laser cut stencil, and paste volumes were measured.

#### **Placement**

A fine pitch placement machine was used for placement of all SMT connectors. Mezzanine connector B was easily picked from tape and reel and placed using standard nozzles. The socket was received packaged in JEDEC trays, and was picked using standard nozzles as well. As the Mezzanine A connectors were received in thermoformed plastic trays, vibratory feeders were used to feed the components into the machine. Two different heights of Mezzanine connector A were included in the project plan. On the motherboard, a 5 mm and a 15 mm receptacle were used. On the mezzanine daughter card, a 10 mm and a 20 mm plug were used. On both the motherboard and the mezzanine daughter card, no difficulties were encountered with the shorter version of the connector.

#### **Reflow**

Profile cards were created for both the Mezzanine card and the Motherboards. Reflow profiles were generated in a 10 zone convection oven, using a nitrogen reflow environment. Representative reflow profiles for the Mezzanine card and the Motherboard are shown in Figures 5 and 6 respectively.

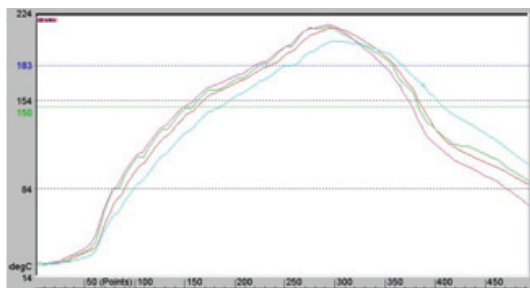


**Figure 5 - Mezzanine Board Reflow**

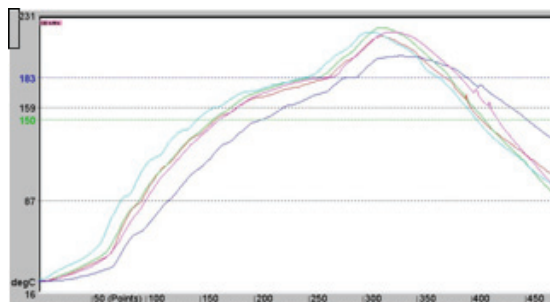


**Figure 6 - Motherboard Reflow Profile**

**Table 2 - Yield Data for BGA Connectors**

Connector	Surface Finish	Number Assembled	Number Passed X-ray
Motherboard			
Socket	ENIG	21	21
Mezzanine A (5mm)	ENIG	32	32
Mezzanine A (15 mm)	ENIG	42	42
Mezzanine B	ENIG	42	42
Mezzanine Daughter Card			
Mezzanine A (10 mm)	OSP	10	10
Mezzanine A (20 mm)	OSP	10	10
Mezzanine B	OSP	10	10
Mezzanine A (10 mm)	ImmAg	32	32
Mezzanine A (20 mm)	ImmAg	42	42
Mezzanine B	ImmAg	42	42
Mezzanine A (10 mm)	ENIG	32	32
Mezzanine A (20 mm)	ENIG	42	42
Mezzanine B	ENIG	42	42

**Rework**

As suggested by IPC-9701, a set of reworked samples was included in the test plan. Ten sites per connector type on each surface finish were selected for rework. Only the taller versions of Mezzanine connector A were reworked, the effect of stack height should be determined from the primary attach sample. With the combination of height and internal construction (increase in metal structure) in the taller mezzanine connector, we suspected that this connector would be the more challenging of the two. Reworked samples are also included in the ATC testing.

**Press Fit Connectors**

Following SMT assembly, the Backplane daughter cards and the motherboard underwent the press fit operation.. Insertion forces were measured, and ten connectors of each type were removed and replaced, and the insertion force of the second placement was measured. The press fit portion of the experiment was also repeated for lead free, with a tin plated connector. On the lead free cell, the Backplane card will remain FR-4, but the motherboard will be made from a high temperature lead free compatible FR4. The press fit cards were then placed into accelerated thermal cycling along with the BGA connectors. Although ATC alone is not a typical reliability test for press fit style connectors, it expected to be a relative measure of the

reliability of the press fit connections on the various surface finishes, and in tin/lead vs. lead free may be made. Limited sample sizes precluded the use of more conventional press fit reliability tests.

### **Card Merge**

Following the completion of the SMT, rework and press fit assembly of the individual cards, the various daughter cards were mated together and mechanicals, such as standoffs and heat sinks, were added. The completed assemblies were then ready for accelerated thermal cycling.

### **Accelerated Thermal Cycling**

Following the completion of assembly and rework, all assemblies, including the lead free press fit boards, were subjected to accelerated thermal cycling to assess their reliability. The completed assemblies were then divided into two thermal cycling chambers. The tin/lead assemblies were placed in one chamber, and the lead free press fit assemblies in the second. Fixtures were created to hold the cards in place inside the chamber, and to allow the air inside the chamber to circulate around them as freely as possible. Figure 7 shows the tin/lead assemblies mounted inside the thermal cycling chamber.



**Figure 7 - Assemblies in Thermal Cycling Chamber**

The standard, preferred thermal cycle from IPC-9701 was selected for use in this testing, and a profile was developed for a 0°C to 100°C cycle, with a total cycle length of 90 minutes for the tin/lead assemblies, and 60 minutes for the lead free press fit assemblies. A quicker profile could not be attained due to the thermal mass and the complex geometry of the assemblies while still meeting the requirements set in IPC-9701. The design attempted to mitigate the impact of these card features on airflow, but it was not entirely possible to eliminate the restrictions to air flow.

All assemblies were in-situ monitored during the test using data loggers. A net was deemed to have failed once 5 consecutive readings showing a 20% or greater increase over the time zero resistance were recorded. The test was stopped periodically to isolate the failing pin(s) on the failed nets to allow failure analysis to be focused on the site of the first failures. The test vehicles were designed to allow each of the connector types to be cut out from the assembly without damaging the connections to the remaining connector types. This allows failure analysis to be conducted as soon as possible after the failures were detected.

### **Torque and Vibration Testing**

A total of thirty Metropolis motherboards were assembled with a topside SMT socket and heatsink assembly, while the bottom side of the board only had the SMT socket attached. Only the topside socket was monitored during testing. Of the thirty motherboards assembled, fifteen assemblies were tested for vibration while the other fifteen assemblies were torque tested. Three surface finishes were used in the test matrix (ENIG, ImmAg, OSP). The data was collected using the 6000 Strain Measurement System. The torque test was based on Celestica's internal specification of between 0.6-0.75 degrees per inch (length of board) for 25 cycles. All fifteen samples tested passed with no resistance increases. Figure 8 illustrates torque test setup. Figure 9 illustrates the resistance measurements observed during torque testing on the different surface finishes tested.

Vibration testing was performed using a LDS V894 vibrating table. Tests were performed based on the supplier's specification for shipping and handling. The test parameters were: 3.13GRMS, random 5Hz-20Hz 0.01 g<sup>2</sup>/Hz sloping up to 0.02g<sup>2</sup>/Hz 20Hz-500 Hz 0.02 g<sup>2</sup> 10 minutes/axis, 3 axis (X, Y and Z). The samples were monitored in-situ for resistance

increases during the test. None of the samples tested exhibited any increase in resistance; therefore all the samples passed the vibration test specified. Figures 10 and 11 show the assemblies under test on the vibration table. The vibration spectrum is shown in Figure 12.

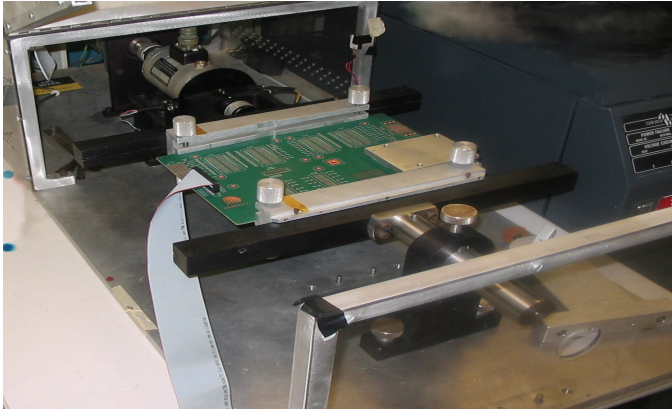


**Figure 8 - Torque Test**

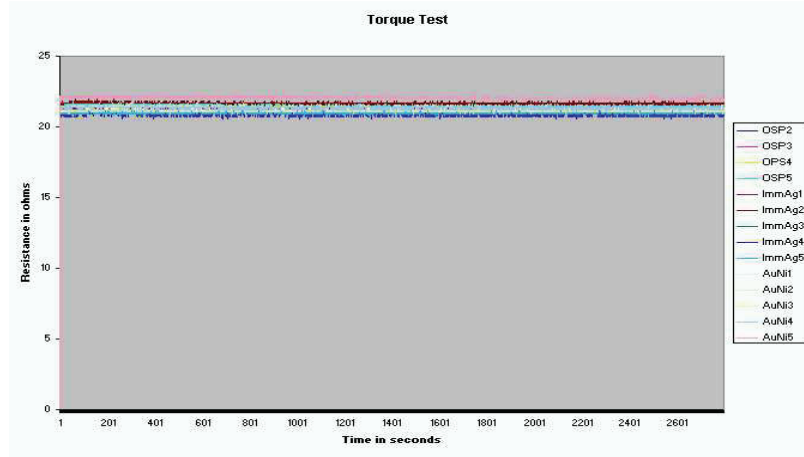


**Figure 9 - Torque Resistance Measurements**



**Figure 10 - Setup of Vibration for X-axis**

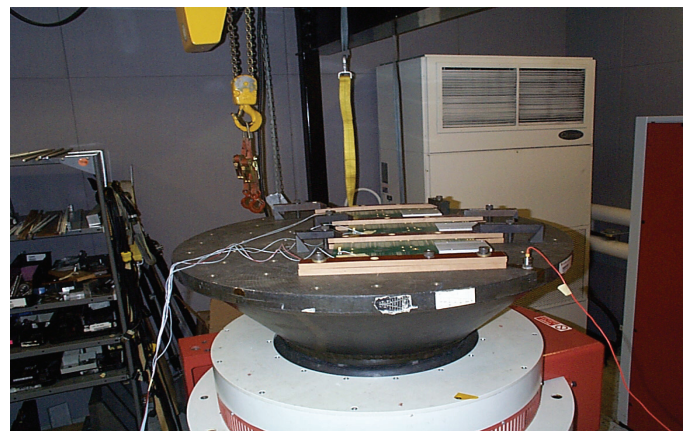


**Figure 11 - Setup of Vibration on Z-axis**

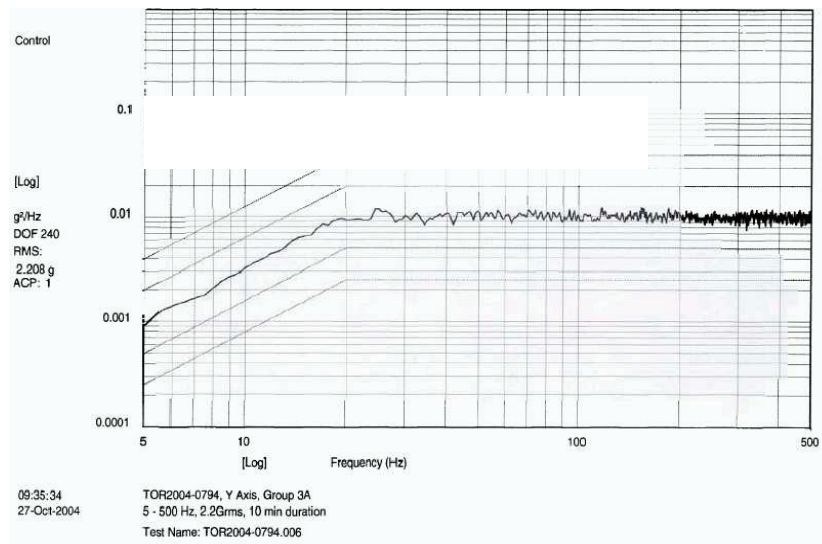


**Figure 12 - Vibration Graph for Y-axis**

## Results

### Mezzanine Connector B

#### Weibull Data

Figure 13 shows the Weibull curves for the primary attach data on each of the three surface finishes. Figure 14 compares the primary attach results to the rework results for ENIG and ImmAg. Figure 14 shows that little difference was found between the three surface finishes. The curve for the OSP samples appears to indicate slightly better reliability, but the sample size was limited and the fit of the curve to the data was not as good as desired. Therefore, it cannot be concluded that OSP was any better than the other finishes.

The slopes of the Weibulls are similar, and range between 4.0 and 5.8. This indicates that the failures are, as expected, solder joint fatigue failures, which will be verified through detailed failure analysis.

Figure 15 shows that for Immersion Silver, the reliability of primary attached and reworked connectors is similar. For ENIG, the characteristic life of primary attach and reworked connectors was very similar, but the slope of the curves was different, dropping from 4.0 for primary attach to 2.2 for the reworks. As a result, the curve indicates that the N1 (number of cycles at which 1% of the population had failed) for reworked connectors would be significantly lower – less than 100 cycles – than for the primary attached connectors, at just over 300 cycles. This result was unexpected and requires additional failure analysis to determine the root cause

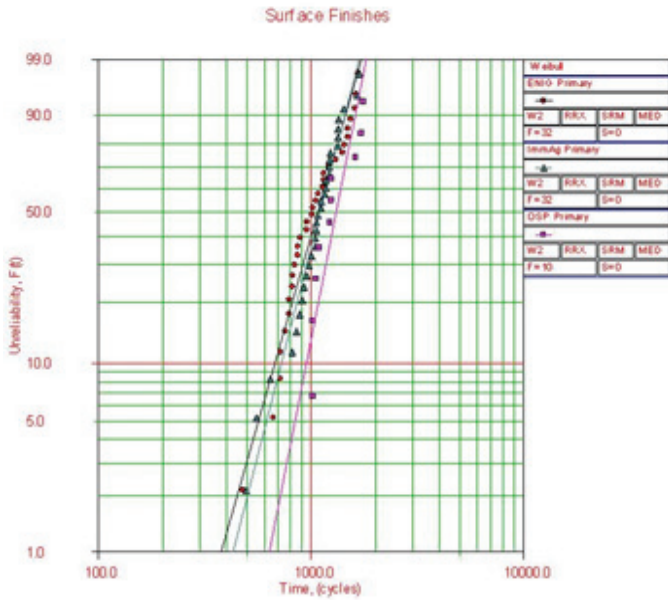


Figure 13 - 2-Parameter Weibull Plots for Mezzanine Connector B on Various Surface Finishes

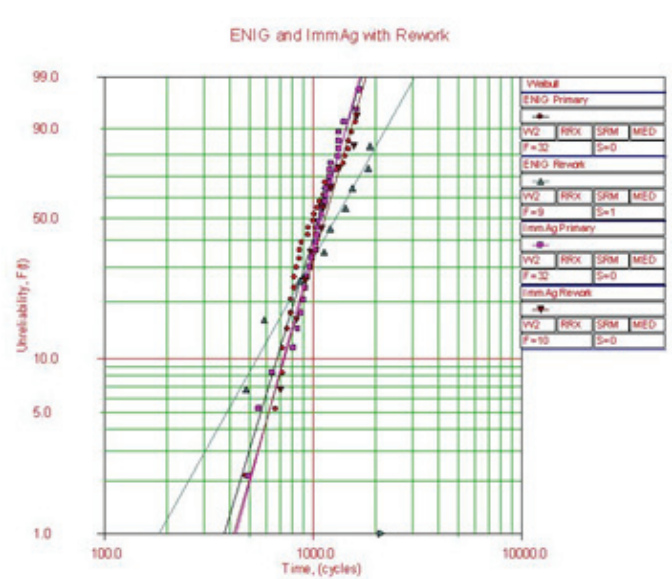


Figure 14 - 2-parameter Weibull plots for Mezzanine Connector B showing Rework vs. Primary Attach

#### Failure Analysis

As each component failed, the location of the failing pin or pins was isolated using a multimeter and recorded. Selected components were then cut out from the test vehicles for further analysis. The procedure for removing a sample from the test was somewhat more complex than for conventional BGA components, as the possibility of contact failures must be taken into consideration. When a sample was identified for removal, the standoff hardware was removed, and then the daughter card was carefully unmated from the motherboard. The contacts attached to each of the pins previously identified as having failed were examined for any signs of contamination or unusual wear. This was done to determine if the increase in resistance observed in testing was due to a contact failure. The section of the motherboard containing the samples of interest was then cut out. If no signs of damage or wear to the contacts were detected, the samples were cross sectioned to determine if the solder joints had failed. The motherboard and daughter card sides were trimmed down and potted in the unmated condition. The sections were made to the first failure locations previously identified using the multimeter, and the failure mode for each sample was determined.

The cross sections revealed that the majority of samples failed on the daughter card side, as shown in Table 3.

**Table 3 - Samples for Cross Sectioning Showing Failure Locations**

Assembly	P105 failed sites	P106 failed sites
OSP 5	A16, H25	H9
ImmAg 13	A19	H15
AuNi 1	H23	H8, H18, H24
AuNi 20	A25	H15, H17, H18
ImmAg 7	A13	H25, H26, H30
ImmAg 20	A19	H9, H14, H16, H23 H25
AuNi 12	A15	A12

Red - Failure on Daughter Card Side  
Green - Failure on Both Sides

The cracks on the daughter card side were found to be typical fatigue failures, though they formed on the board side of the joint rather than the component side. This is likely due to the unusual ball attach method at the component side – the balls are not soldered to flat pads as they would be in a conventional BGA package, but rather are reflowed onto pins which form part of the contacts. The cracks observed in the failed joints propagated through the bulk solder above the intermetallic layer on the board side. Figure 15 shows typical joints before ATC, with the board side pad and component side connections visible, and Figure 16 shows a typical failed ball on the daughter card.

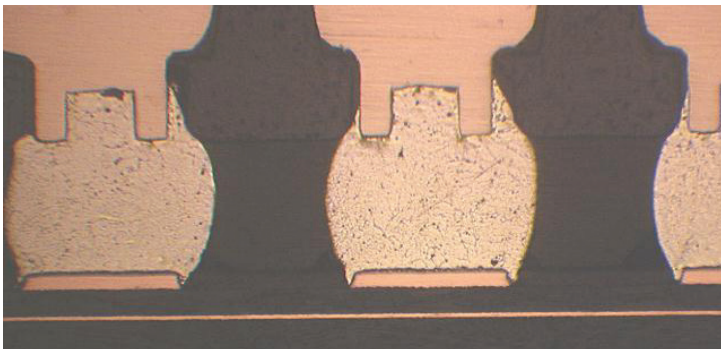


**Figure 15 - Typical Time Zero Mezzanine Connector Solder Joint**

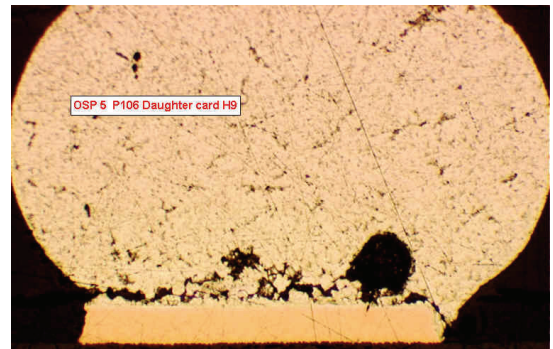


**Figure 16 - Typical Solder Joint Failure on Daughter Card**

In four cases, it was found that there were cracks on both the Motherboard side and the Daughter Card side. In each case, there was a similar fatigue crack on both sides, again, along the PCB side of the joint. Figures 17 and 18 shows one example of these failures.

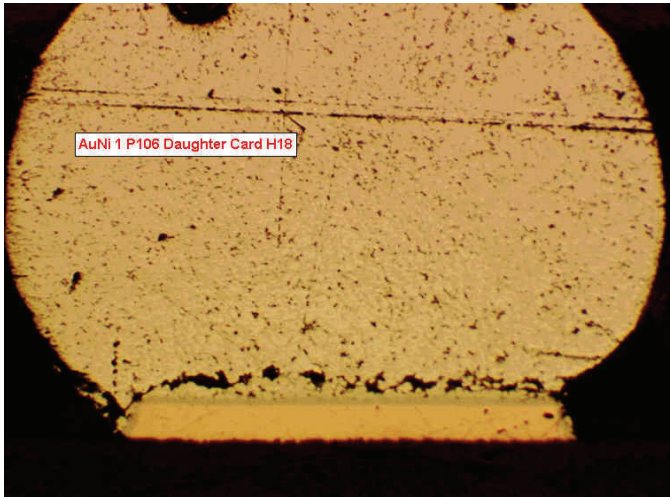


**Figure 17 - Typical Solder Fatigue on Motherboard**

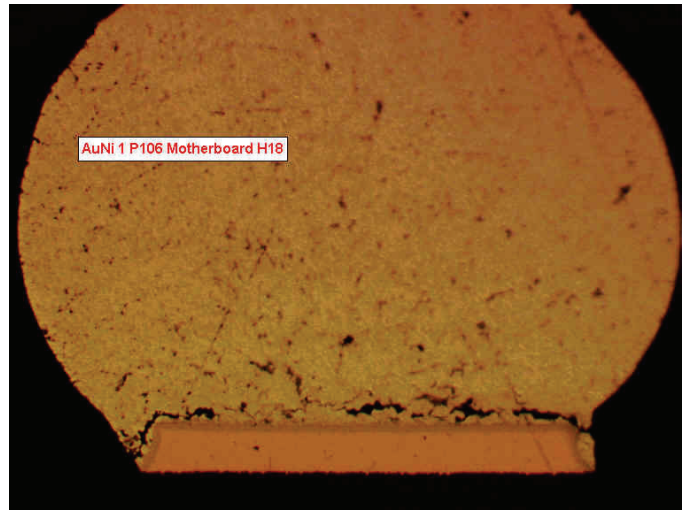


**Figure 18 - Typical Solder Fatigue on Daughter Card**

As the failure locations were isolated and documented, it became clear that the failures were occurring in a variety of locations that exhibited a vague pattern. To assist in understanding the failures, a map of the locations of these first fails was plotted for each connector site and each surface finish. These are seen in Figures 19 through 21. The diagrams show the number of times a pin was indicated as a failure when first probed. It must be noted that for many connectors, more than one failing ball was identified when first probed. The sample size for ENIG and Immersion Silver is the same, but is smaller for OSP due to the smaller number of OSP assemblies built. In addition, these diagrams show the primary attach data only, so the sample sizes are not equal between site P105 and P106. It is therefore important to consider the general trends in failure location identified in these diagrams rather than the actual number of failures recorded. Each diagram shows both the P105 and P106 locations of Mezzanine Connector B relative to the outline of the daughter card used to complete the daisy chains. Standoff locations are indicated by the white circles in the daughter card corners.

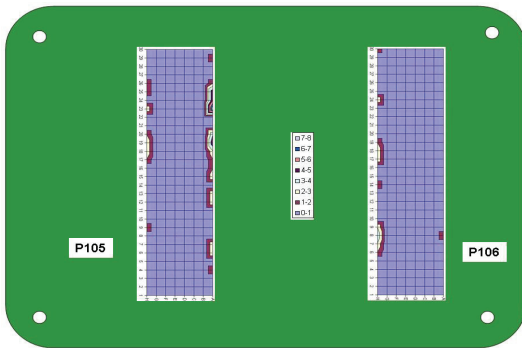


**Figure 19 - Location Map of First Failures for Mezzanine Connector B on ENIG**

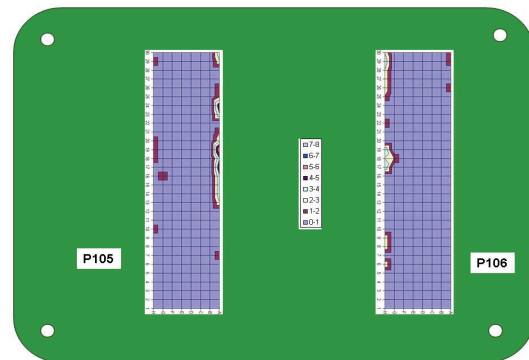


**Figure 20: Location map of first failures for Mezzanine Connector B on ImmAg**

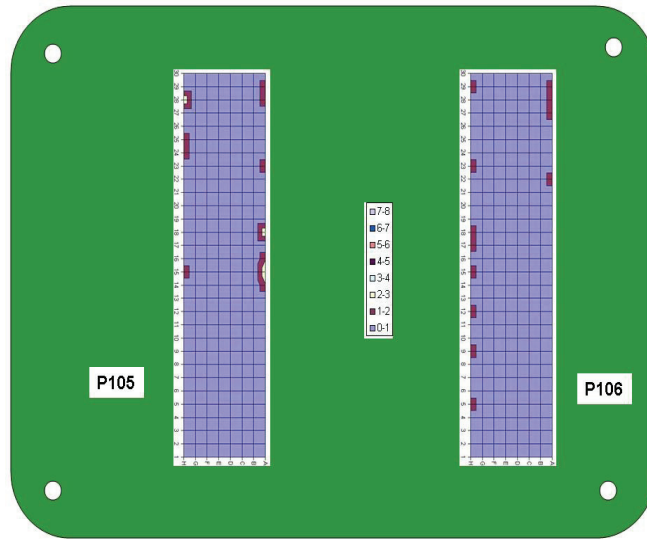


**Figure 21 - Location Map of First Failures for Mezzanine Connector B on OSP**

As can be observed from the above diagrams the failures are not limited to the distance from the neutral point, as is expected. The failures tend to be concentrated along the length of the connectors, with some tendency to cluster near the middle of the long edge. Another somewhat unexpected observation was that the failures did not occur symmetrically on both long edges of the connector. Surface finish did not appear to a factor on the failure location. Similar trends were observed for the reworked cards – Figure 22 shows the failure location map for the primary attach and reworked samples on ImmAg. As no strong dependency on surface finish was observed in the rework failure locations, the ENIG rework failure map is not shown.

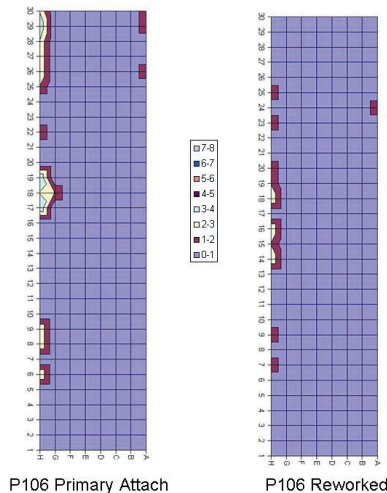


**Figure 22 - Location Map of First Failures for Mezzanine Connector B, Primary Attach vs. Reworked**

Further investigations were undertaken to determine why the failures appeared where they did. CTE measurements had previously been made on a connector from the Mezzanine Connector B product family. The connector was the same footprint as the Receptacle currently under test, but was slightly larger in height. Samples of the plastic housing material were removed and the CTE was measured by Digital Speckle Correlation [5][6]. These measurements determined that the CTE of the connector was different in the x, y and z directions, which was due to the flow of the polymer material during the molding process. It was determined that the CTE in the x direction, measured near the centre of the connector, was approximately 15ppm/°C. This closely matches the value of 13-14 ppm/°C measured on the Metro motherboard. However, in the y direction, the CTE of the connector was higher, in the range of 23-27 ppm/°C. In the y direction, therefore, there is a CTE mismatch between the board and the connectors. This would tend to drive the failures to form along the long edges of the connector, as was observed from the testing. But this alone does not fully explain why the failures were concentrated on the inside edges of the connectors, or why they appeared primarily on the daughter card side.

It was noted from the same connector CTE measurements that the CTE in the z direction was relatively high – in the range of 84 to 97 ppm/°C. The CTE of stainless steel, the material used for the standoffs was found to be 10-17 ppm/°C, from reference documents. Figure 23 shows a simple diagram of the Mezzanine Connector B portion of the assembly in cross section. The relevant CTE values are shown for the various components of the system.

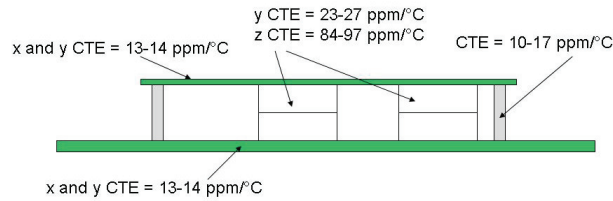


**Figure 23 - CTE Values for Various Components of the Mezzanine Connector B Assembly**

Based on these CTE numbers, it is theorized that the system behaves as follows. As the assembly is heated up, the connectors begin to expand in the z-direction. The standoffs also begin to expand, though not as far due to their lower CTE. As the daughter card is thinner and more compliant than the motherboard, it begins to bow upwards as the connectors continue to expand, and a tensile stress is created in the card. Simultaneously, the daughter card, motherboard, and connectors expand in the x- and y- directions. These key movements are shown in Figure 24.

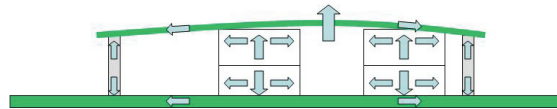


**Figure 24 - Key Movements Contributing to Failures**

On a solder joint level, this would indicate that the failures would occur primarily on the daughter card side due to the displacement of the daughter card and tensile stress. Figure 25 shows a simplified diagram of one half of the daughter card showing the key stresses on the solder joints. A tensile stress is generated through the daughter card as described above, and is represented by the large arrows above the card in this figure. As the connector CTE in the y-direction exceeds the CTE of the board, the connector will expand at a greater rate than the board. The resultant stress is represented by the smaller arrows in the connector body.

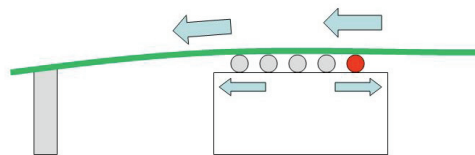


**Figure 25 - Summary of Key Stresses on Daughter Card Solder Joints**

The result is that on the outside row of balls (closest to the standoff), the tensile stress in the card and the stress from the expansion of the connector act in the same direction, and the solder joint experiences a relatively lower strain. On the inner row (represented by the red solder joint), the tensile stress in the card and the stress from the expansion of the connector relative to the board act in opposite directions, resulting in a higher strain on the solder joint. As a result, the inner rows of balls would tend to fail first, which is what was seen from the ATC results.

Based on this theory, it is thought that using standoffs of a material more closely matching the z-direction CTE of the connectors may distribute the stresses on the joints more evenly and may result in a longer fatigue life. This would require verification in a future test.

Mezzanine A

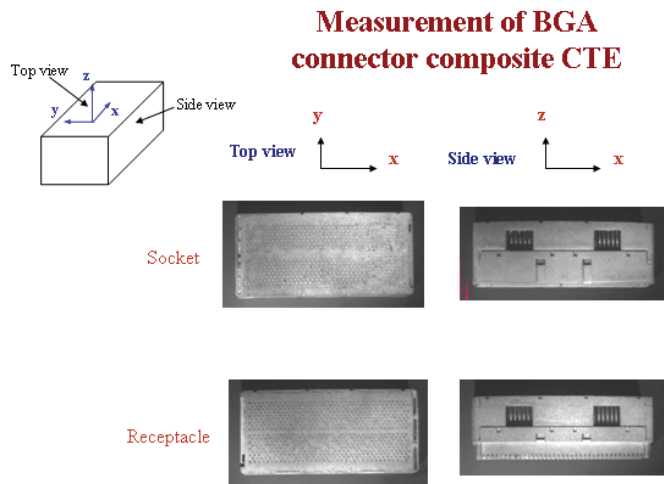
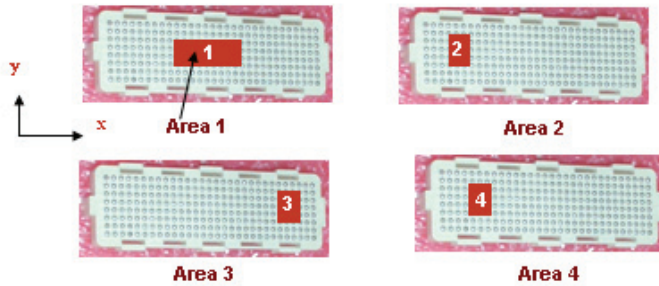


Table 5- CTE Measurements of Mezzanine Connector A

Direction	CTE ppm/°C	
	Socket	Receptacle
x	23	19
y	21	22
z	63	46

Figure 26 - CTE measurement areas of Mezzanine

## Mezzanine B



**Table 6 - CTE Measurements of Mezzanine Connector "B"**

Area	x	y	z (thickness direction)
1	21	60	
2	10	53	
3	29	48	85
4	13	61	

**Figure 27 - CTE Measurement Areas of Mezzanine Connector "B"**

### Mezzanine Connector Results

Figures 26 and 27 illustrate the locations on the connectors where the CTE measurements were collected by Digital Speckle Correlation method on the Mezzanine connectors.

As can be seen from Table 5, the y-direction (short side of connector) the CTE measured for the "A" type Mezzanine connector was measured to be 21, which is much closer to the CTE of the printed wiring board  $\sim 17\text{ppm/C}$ . Unlike the Mezzanine B connector, the CTE in the y-direction was measured at  $50\text{ppm/C}$  (Table 6). This profound mismatch is the reason on the poor reliability results of this connector versus the larger "A" type mezzanine connector. Secondly, the effect of the pin connection and connector height was another factor that had a profound effect on reliability as illustrated in Figure 28.

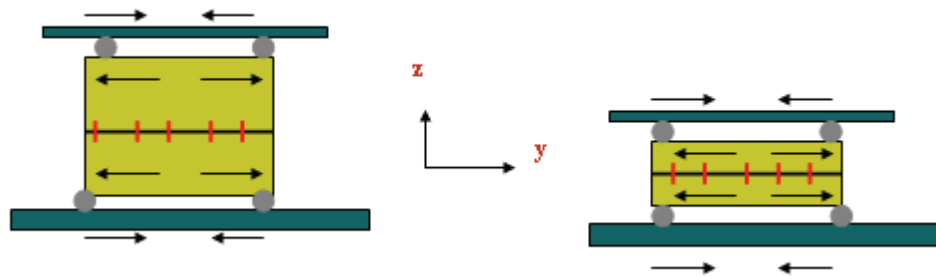


**Figure 28 - Pin Connection and Connector Height of Effect of Mezzanine Connector "A"**

### Results for Other Connector Types

At the time of writing, 4200 cycles of ATC had been achieved. There have been a couple of hard failures on the socket. The failures occurred between 3100 and 3600 cycles. Failures were isolated to the peripheral row of joints located in the middle of the socket. Both A type mezzanine connectors have shown no electrical failures during this time. Data collection on the two press fit connector types showed that 3 sets of the total set of 20 reworks failed. The failures occurred in the vicinity of 1500 cycles. The failure sites were isolated in all instances and seem to be totally random at this time. The press fit connectors which were from initial attach have intermittent failures but isolation could not be verified at room temperature. Thermal cycling will continue until 6000 cycles. In depth analysis on failed or intermittent sites will be performed at this time.

### Conclusions

As signal frequencies increase, designers are faced with difficult choices on selecting reliable interconnects for their products. With this in mind, one may choose a part based on their previous knowledge of similar technologies. Such may be the case, when a designer is faced with using area array connectors. As this paper illustrated there are many other factors to consider when using area array interconnects to their component counterparts. In area array components, failures usually occur at the farthest distance from the neutral point or at the edge of the die. As illustrated the Mezzanine Connector "B" presented a different failure mode than an area array component. The failure mode was dependent on both the assembly geometry and the

material properties of the standoffs, yet these same dependencies did not affect the reliability of the “A” type Mezzanine connector.

As interconnects become more complex in both structure and materials, second level testing is absolutely necessary to ensure product reliability. It is highly recommended that testing be performed on product by product basis to fully understand the stresses present on each interconnect type.

### **Acknowledgements**

The authors gratefully acknowledge Dr. Hua Lu of Ryerson University, and his staff and students, for the CTE measurements of Mezzanine Connector B by Digital Speckle Correlation.

The authors also wish to thank the connector and processor suppliers who contributed components to this project.

Finally, the authors wish to thank Blake Harper of Celestica for the Weibull plots, and Russell Brush and Jeffrey Tang of Celestica for assistance with the accelerated thermal cycling and data collection.

### **References**

- [1] McCormick, Heather, George Riccitelli and Jullie Tran, “Evaluating the Manufacturability and Reliability of New Connector Designs”, Proceedings of SMTA International, 2004, pp. 258-263.
- [2] IPC, "IPC-9701 Performance Test Methods and Qualification Requirements for Solder Mount Attachments" January 2002.
- [3] NEMI “NEMI Technology Roadmaps – 2002 Edition”, December 2002.
- [4] Prismark Partners LLC “Wowie ZAUI - Connections at High Speed” September 2002.
- [5] Lu, Hua, “Applications of Digital Speckle Correlation to Microscopic Strain Measurement and Materials Property Characterization”, Journal of Electronic Packaging, 1998, pp. 275-279.
- [6] Vogel, D et al. “Determination of Packaging Material Properties Utilizing Image Correlation Techniques”, Journal of Electronic Packaging, 2002, pp. 345–351.